

## COPRECIPITATES OF Cd, Cu, Pb AND Zn IN IRON OXIDES: SOLID PHASE TRANSFORMATION AND METAL SOLUBILITY AFTER AGING AND THERMAL TREATMENT

CARMEN ENID MARTÍNEZ AND MURRAY B. MCBRIDE

Department of Soil, Crop, and Atmospheric Sciences, Cornell University, Ithaca, New York 14853, USA

**Abstract**—Solid phase transformation and metal solubility were monitored after coprecipitation of Cd<sup>2+</sup>, Cu<sup>2+</sup>, Pb<sup>2+</sup> and Zn<sup>2+</sup> with Fe<sup>3+</sup> to form ferrihydrite by titration to pH 6. The (co)precipitates were aged at room temperature for up to 200 d and subsequently heated for 60 d at 70 °C. The mode of (co)precipitate formation, rapid and slow titration, was also investigated. Metal solubility was measured by anodic stripping voltammetry. Surface area, Fourier transform infrared (FTIR) and X-ray diffraction (XRD) analysis were used to follow the transformation of ferrihydrite after initial (co)precipitation. Electron microprobe analysis (EMPA) was used to show the distribution of metals within ferrihydrite aggregates. Thermal treatment produced a reduction in soluble Cd<sup>2+</sup> and Zn<sup>2+</sup>, whereas Pb<sup>2+</sup> appeared to be expelled from the solid phase. The more stable coprecipitate (formed by slow titration) maintained a constant Cu<sup>2+</sup> solubility after thermal treatment. Characterization of the solid phase by XRD indicated that the presence of low levels of metals did not affect the initial or final transformation products, although metals present during the slow titration seemed to stabilize a higher surface area material. The rapid titration resulted in a less ordered (1-line) ferrihydrite than the slow titration (9-line). Furthermore, FTIR analysis indicated that the presence of metals promoted the formation of mixed (microcrystalline) end-products. The initial coprecipitation products seem to determine the final thermal transformation products. These transformation products include ferrihydrite, hematite (Hm), and goethite (Gt)- and lepidocrocite-like microcrystalline structures. Although experimental conditions were favorable for the homogeneous distribution of metals throughout the coprecipitate, EMPA suggests that Cu and Zn segregation within aggregates of Fe oxides occurs.

**Key Words**—Aging Study, Coprecipitation, Electron Microprobe Analysis, Ferrihydrite Transformation, Metal Solubility, Rate of Titration, Thermal Treatment.

### INTRODUCTION

Ferrihydrite is one of the soil components that contributes to the retention of trace metals in soils. Thermodynamic principles suggest that among the mechanisms involved in the removal of trace elements from solution, coprecipitation will often result in the lowest metal solubility. Thus, metal coprecipitates with Fe oxides could limit their toxicity and (bio)availability in soils. Evidence exists for Cd<sup>2+</sup>, Cu<sup>2+</sup>, Pb<sup>2+</sup> and Zn<sup>2+</sup> incorporation into noncrystalline Fe oxides by coprecipitation (Kinniburgh et al. 1976; Crawford et al. 1993; Spadini et al. 1994; Ford et al. 1997). The dynamic nature of a freshly precipitated material such as noncrystalline Fe oxide, however, can result in long-term changes in metal solubility after aging and/or transformation of the original product into a well-crystallized material. For instance, a Cu-ferrihydrite coprecipitate formed at room temperature and later aged at 98 °C was found to increase %Cu removal (Kolthoff and Moskovitz 1937). This was interpreted as Cu entering the precipitate with increasing time of heating, thus suggesting its incorporation into the aging Fe hydrous oxide. In another study, Ford et al. (1997) found that coprecipitated Pb and Cd became less extractable after ferrihydrite transformation to goethite. Conversely, an adsorption/reversibility study indicated that Cd

adsorption at pH 7 becomes somewhat less reversible with aging, while no changes were observed for Pb (Ainsworth et al. 1994). It was suggested that Cd is incorporated into the recrystallizing oxide structure.

It is known that ferrihydrite phase transformation results in the formation of mixed end-products. Schwertmann and Murad (1983) found that 50% of ferrihydrite was converted to Gt and Hm at pH 5–6 and ambient temperature (24 °C) after 150–200 d of aging. The composition of the Gt-Hm mixture did not change considerably over a period of 15 mo to 3 y. Lepidocrocite formation from ferrihydrite has also been reported to occur under slightly acidic (pH 6) conditions (Cornell et al. 1989).

The nature of ferrihydrite transformation products formed by aging depends on factors including pH, temperature and the presence, quantity and identity of foreign ions. In studying the effect of pH on the formation of Gt and Hm from ferrihydrite, Schwertmann and Murad (1983) found that the formation of a highly crystalline Hm was favored at pH 6 while a crystalline Gt was formed at pH 5. Metal cations tend to retard ferrihydrite transformation when present at high metal/(metal + Fe) mole ratios. Coprecipitates of Si, Cu, Co and Mn with Fe to form ferrihydrite are shown to retard the rate of ferrihydrite transformation to more crystalline phases (Anderson and Benjamin 1985; Cor-

nell and Giovanoli 1987; Cornell and Giovanoli 1988; Cornell and Giovanoli 1989), with the retardation effect of metals following the order:  $\text{Cu} \gg \text{Co} \gg \text{Mn}$ . The presence of divalent cations, such as Cu, was also shown to increase the proportion of Hm relative to Gt, thus influencing the nature and quantities of the more crystalline end-products formed (Cornell and Giovanoli 1987, 1988, 1989). Metals can prevent Gt formation by interference at 2 stages: 1) by retarding dissolution of ferrihydrite, and 2) by hindering nucleation and growth in solution.

The influence of divalent cations on ferrihydrite aging and transformation have often been evaluated under conditions that are not realistic for soil environments, namely, very alkaline pH ( $\sim 12$ ), high metal/(metal + Fe) mole ratios, and/or high (70 °C) temperatures (Cornell 1988; Cornell and Giovanoli 1988; Cornell et al. 1989). This study investigates the effect that simultaneous coprecipitation of low levels of  $\text{Zn}^{2+}$ ,  $\text{Cd}^{2+}$ ,  $\text{Pb}^{2+}$  and  $\text{Cu}^{2+}$  with  $\text{Fe}^{3+}$  to form ferrihydrite has on the end-products formed after aging for up to 200 d at room temperature (23 °C) and at pH values between 5 and 6. Thermal treatment (60 d at 70 °C) of the coprecipitates followed this long-term aging period. As ferrihydrite phase transformation can affect the solubility of metals initially present in the coprecipitate, soluble  $\text{Zn}^{2+}$ ,  $\text{Cd}^{2+}$ ,  $\text{Pb}^{2+}$  and  $\text{Cu}^{2+}$  are measured during its transformation. The effect that preparation conditions (rapid or slow titration) have on the coprecipitates formed initially, their transformation products and metal solubility is also examined. The spatial distribution of Cu and Zn within Fe oxide aggregates is determined at a microscopic level by EMPA.

#### MATERIALS AND METHODS

Solutions containing  $4.95 \times 10^{-3} \text{ M Fe}^{3+}$ ,  $3.91 \times 10^{-7} \text{ M Cd}^{2+}$ ,  $1.04 \times 10^{-5} \text{ M Cu}^{2+}$ ,  $1.1 \times 10^{-6}$  or  $3.3 \times 10^{-6} \text{ M Pb}^{2+}$  and  $2.02 \times 10^{-5} \text{ M Zn}^{2+}$  in 1 mM  $\text{KNO}_3$  background electrolyte were titrated rapidly ( $6.24 \text{ mL min}^{-1}$ ) and slowly ( $0.03 \text{ mL min}^{-1}$ ) with 0.1 M KOH until the pH reached 6. The concentrations used represent loadings of: 0.004 mol  $\text{Zn}^{2+}/\text{mol Fe}^{3+}$ ,  $7.9 \times 10^{-5}$  mol  $\text{Cd}^{2+}/\text{mol Fe}^{3+}$ , 0.0002 or 0.0006 mol  $\text{Pb}^{2+}/\text{mol Fe}^{3+}$  and 0.002 mol  $\text{Cu}^{2+}/\text{mol Fe}^{3+}$ ; all 4 metals in combination were coprecipitated with  $\text{Fe}^{3+}$  for a total of 0.0065–0.0069 mol  $\text{M}^{2+}/\text{mol Fe}^{3+}$ . These values represent the maximum concentrations in the Fe oxide if complete retention occurred. Ferrihydrite transformation and metal solubility were studied after 2 different rates of coprecipitate formation. In many coprecipitation studies, the pH of the system is raised rapidly, creating artifacts due to localized high alkalinity during titration. Thus, a slower rate of titration was also studied in an attempt to simulate more natural conditions and possibly avoid artifacts. Control experiments, representing both rapid and slow titration,

were conducted to obtain a precipitate without trace metals by titrating a  $4.95 \times 10^{-3} \text{ M Fe}^{3+}$  solution with 0.1 mM KOH in the same manner as described above.

Once the coprecipitates were formed, and at time intervals ranging from 0 to 200 d, soluble  $\text{Cd}^{2+}$ ,  $\text{Cu}^{2+}$ ,  $\text{Pb}^{2+}$  and  $\text{Zn}^{2+}$  were determined simultaneously by differential pulse anodic stripping voltammetry (dpasv) after an aliquot of the suspensions was centrifuged (10 min at 15,000 rpm), and the supernatant filtered (0.2  $\mu\text{m}$  polycarbonate membrane filter) and acidified (1 M HCl). The (co)precipitates collected at various time intervals were freeze-dried and kept for further analysis. Surface area, FTIR and XRD analysis were used to follow the process of aging, crystallization and transformation of ferrihydrite after its initial (co)precipitation. Surface area (BET) was determined by 3-point  $\text{N}_2$  adsorption measurements after an outgas procedure with dry  $\text{N}_2$  of 1 h at 100 °C. IR spectra were obtained using a pellet containing 2 mg of sample mixed with 170 mg of KBr. Measurements were made using a Fourier Transform Perkin-Elmer 1720-x spectrometer at 2  $\text{cm}^{-1}$  resolution and 100 co-added scans. XRD analyses were made using a Scintag, Inc., theta-theta diffractometer with a solid-state intrinsic germanium detector.

After about 200 d of aging at room temperature, aliquots of the suspensions were heated for 60 d at 70 °C to accelerate ferrihydrite phase transformation. All samples had a pH of about 5.4 at the time this thermal treatment was initiated. After the samples were heated for 60 d, the pH had dropped to 3.54–4.16. Thus, at the end of the thermal treatment, the pH of the suspensions was adjusted to the same value as before heating (pH  $\sim 5.4$ ), the suspension centrifuged and the supernatant filtered and acidified. Soluble metals were then analyzed by dpasv, and the solid phase characterized by surface area, FTIR and XRD analysis as described previously.

EMPA of the coprecipitates was employed to determine Cu and Zn distribution in the solid phases present immediately after coprecipitate formation ( $t = 0$ ), after 200 d of aging at room temperature and after thermal treatment. Cadmium and Pb distribution could not be determined, since Cd concentration in/on the solid phase was below  $100 \text{ mg kg}^{-1}$  and Pb background signal was high and interfered with its accurate determination. Iron was also measured to ensure that an Fe oxide particle was analyzed. The solid particles were embedded in epoxy resin and polished until a relief-free flat surface was apparent. Successive polishing steps employed a 600-grit wet abrasive paper, 6- $\mu\text{m}$  and 1- $\mu\text{m}$  diamond suspensions and a 0.05- $\mu\text{m}$   $\text{Al}_2\text{O}_3$  suspension. The samples were then cleaned in an ultrasonic cleaner, air-dried and carbon coated. Line-scans were carried out using a wavelength dispersive spectrometer (WDS) attached to a JEOL 733 Superprobe operated at 25 kV and 100 nA. Counts were

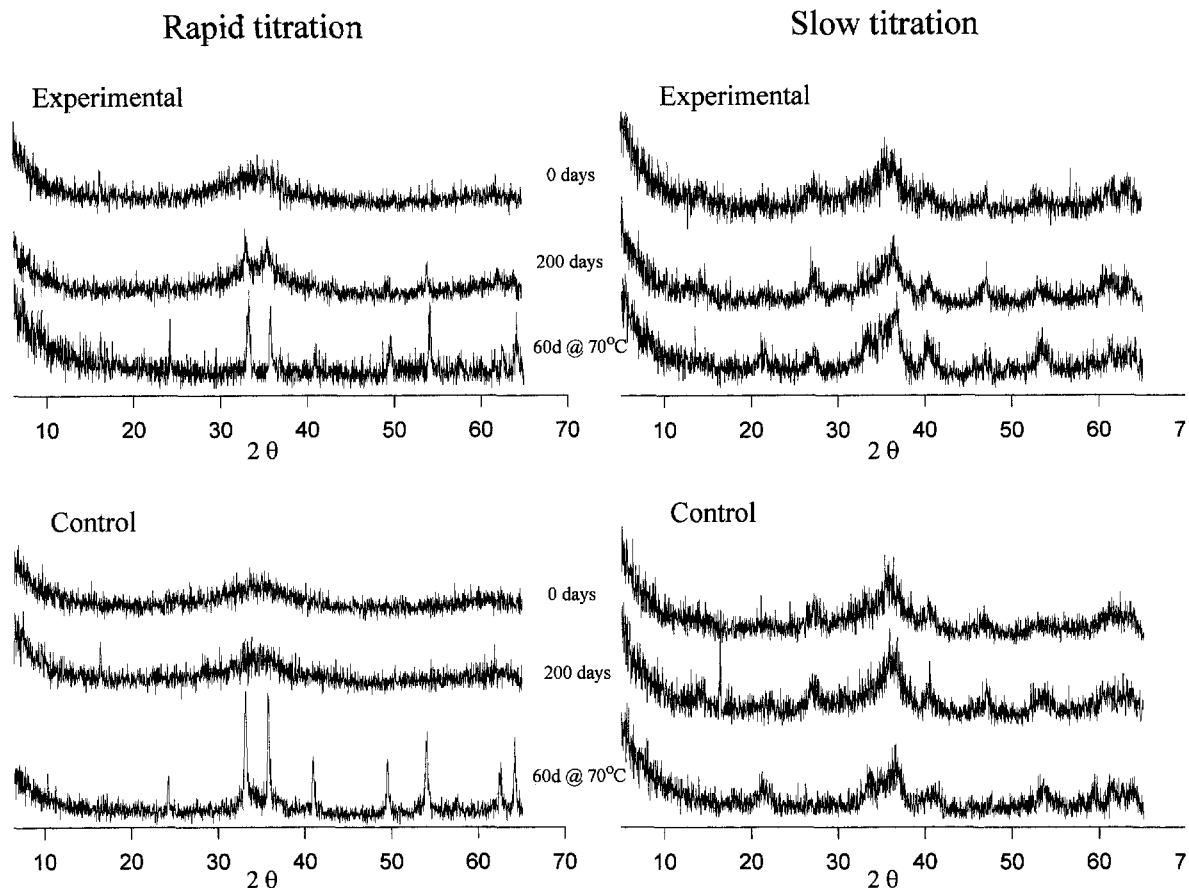


Figure 1. XRD patterns of (co)precipitates taken immediately after their formation ( $t = 0$  d), after aging for 200 d at room temperature and after thermal treatment (60 d at 70 °C).

accumulated for 40 s for electron beam line and background scans of Fe, Cu and Zn; background scans were subtracted from electron beam line scans. Several (10–15 per sample) Fe oxide aggregates, selected at random, were analyzed on a 100- $\mu\text{m}$  grid with a 1- $\mu\text{m}$ -diameter electron beam. Thus, the interaction volume was 1  $\mu\text{m}^3$ , and although escape depths of secondary X-rays would depend on sample thickness, this contribution is negligible compared to the actual counts. Additionally, photographs of Fe oxide aggregates were taken using a LEICA 440 scanning electron microscope (SEM).

## RESULTS AND DISCUSSION

### Aging and Thermal Transformation of Ferrihydrate

**SURFACE AREA.** Surface areas of the (co)precipitates did not change in any systematic way during the 200 d of aging at room temperature. The experimental treatments had an average surface area of ( $\text{m}^2 \text{g}^{-1}$ ):  $199 \pm 15$  for the rapid titration, and  $182 \pm 27$  for the slow titration. The control treatments had an average surface area of ( $\text{m}^2 \text{g}^{-1}$ ):  $256 \pm 37$  for the rapid titration,

and  $185 \pm 19$  for the slow titration. All these values are typical of a noncrystalline oxide material. After thermal treatment (60 d at 70 °C), the surface area of the rapidly titrated coprecipitate was reduced to that of a crystalline material ( $25.4 \text{ m}^2 \text{g}^{-1}$ ), while the slow titration seemed to stabilize a high surface area material ( $161 \text{ m}^2 \text{g}^{-1}$ ). Heating the precipitates with no metal (control) reduces their surface area to some extent, but values are still those of a noncrystalline material;  $144 \text{ m}^2 \text{g}^{-1}$  for the rapid, and  $131 \text{ m}^2 \text{g}^{-1}$  for the slow titration. Surface area changes after thermal treatment indicate that a more stable (co)precipitate was formed during the slow titration, which then resisted crystallization during heating. However, no changes in metal solubility could be related in any simple way to these surface area measurements.

**X-RAY DIFFRACTION.** The mode of preparation, rapid or slow titration, results in the formation of noncrystalline materials that differ in degree of order (Figure 1). The formation of these initial products is quite similar in the experimental and control treatments. A 1-line ferrihydrate forms immediately ( $t = 0$ ) after the rapid

titration in both control and experimental treatments. This noncrystalline material is transformed into Hm after heating the suspension for 60 d at 70 °C (Figure 1). A 9-line ferrihydrite forms after the slow titration in both control and experimental treatments (Figure 1). XRD shows no evidence of a well-crystallized Fe oxide even after the heating treatment, although several broad lines appear at  $2\theta$  positions corresponding to Gt (4.18, 2.69, 2.45 Å), Hm (2.70, 2.52, 1.85, 1.70 Å), and lepidocrocite (6.26, 3.29, 2.47, 1.94 Å). Although there is uncertainty regarding the structure of ferrihydrite, it is believed to be composed of tiny (30–70 Å) spherical particles that may have a few layers thick of Hm- or Gt-like order. Again, the slow titration seems to produce a more stable (co)precipitate as evidenced by XRD. The presence of the low mole fractions of  $\text{Cd}^{2+}$ ,  $\text{Cu}^{2+}$ ,  $\text{Pb}^{2+}$  and  $\text{Zn}^{2+}$  did not affect the initial Fe oxide material formed or its final transformation products after (co)precipitate formation by slow titration (Figure 1). Nonetheless, the XRD pattern of the coprecipitate formed by rapid titration indicates the presence of Hm after 200 d of aging at room temperature. Thus, after rapid titration, the metals seemed to accelerate the kinetics of ferrihydrite transformation as evidenced by surface area and XRD analysis (Figure 1). In contrast, a study by Cornell and Giovanoli (1988) showed that low levels of  $\text{Cu}^{2+}$  ( $10^{-4}$  M) at high pH (12.2) had no effect on the kinetics of ferrihydrite transformation and that Gt formation was favored. Because of the extreme pH of that study, comparison to the results reported here is probably unwarranted.

X-ray analysis of the slowly titrated (co)precipitates do not show any well-defined peak after thermal treatment. Although the XRD features of the final products of treatments and controls are very similar, the presence of metals seems to produce broad lines at  $2\theta$  positions corresponding to lepidocrocite (3.29, 1.94 Å). Those broad lines are not present in the control after thermal treatment (Figure 1).

**IR SPECTRA.** The rapid and slow titrations resulted in similar FTIR spectra for coprecipitates and the control precipitate once the system reached pH 6 ( $t = 0$ ), yet the control precipitate formed by rapid titration has a less defined spectrum (Figure 2). No changes in the FTIR spectra were observed during the first 200 d of aging at room temperature for any of the treatments, although intensification of the lepidocrocite bands (1170 and 1026  $\text{cm}^{-1}$ ) may have occurred after slow titration (Figure 2). In the presence of  $\text{Cd}^{2+}$ ,  $\text{Cu}^{2+}$ ,  $\text{Pb}^{2+}$  and  $\text{Zn}^{2+}$ , and after thermal treatment, the coprecipitate formed by slow titration presents IR bands indicative of Gt (896 and 796  $\text{cm}^{-1}$ ), lepidocrocite (1170 and 1026  $\text{cm}^{-1}$ ) and Hm (570 and 480  $\text{cm}^{-1}$ ); IR bands corresponding to Gt, and particularly Hm, dominate the spectrum produced by rapid titration (Figure 2). There is no evidence of the presence of lepidocrocite

in the control treatment after heating the suspensions (rapid and slow titrations). Thus, as evidenced by FTIR analysis, the presence of metals at very low mole fractions does not retard ferrihydrite transformation, but rather promotes the formation of mixed end-products (Figure 2). Coprecipitation of ferrihydrite (at alkaline pH) with single metals (at 9 mole%) has demonstrated that Cu favors Hm formation while Zn favors Gt (Cornell 1988). It was suggested by the authors that in both occasions ferrihydrite was stabilized against dissolution.

Evidence from surface area, IR and XRD analysis indicates that ferrihydrite transformation results in a combination of Fe oxides that differ in degree of crystallinity. It also reveals that Gt-like and lepidocrocite-like microcrystalline structures are present, but they are not well-enough ordered to produce a sharp XRD pattern. The mode of preparation determines the identity and stability of the initial (co)precipitate, and thus, the transformation products. The rapid titration promotes hematite crystal growth while microcrystalline structures are favored by the slow titration. The effect of differences in the rate of titration are more important to determining the final product than the presence of metals. In the laboratory, Hm synthesis is favored at pH 6–9 while Gt forms preferentially at higher or lower pH, and higher temperatures favor Hm formation (Schwertmann and Taylor 1989). However, a slow rate of titration, which could be more representative of natural conditions, could substantially alter the products likely to form in the soil environment. This variable should be given as much attention as pH and temperature in Fe oxide crystallization reactions.

#### Metal Solubility and Distribution During Ferrihydrite Phase Transformation

**METAL SOLUBILITY.** The simultaneous coprecipitation of  $\text{Cd}^{2+}$ ,  $\text{Cu}^{2+}$ ,  $\text{Pb}^{2+}$  and  $\text{Zn}^{2+}$  with  $\text{Fe}^{3+}$  to form ferrihydrite results in variable concentrations of these metals remaining in solution (Table 1). Although  $\text{Cu}^{2+}$  solubility appeared to respond to pH changes during aging at room temperature ( $\text{Cu}^{2+}$  solubility tended to increase as aging decreased pH), soluble  $\text{Cd}^{2+}$  and  $\text{Zn}^{2+}$  were virtually unaffected by the pH changes induced by aging (Martínez and McBride 1998). Less  $\text{Zn}^{2+}$  remains in solution from the coprecipitate formed by slow titration; however, the overall behavior is similar independent of the rate of titration. Decreased  $\text{Zn}^{2+}$  solubility is indicated after 200 d; a further decrease occurs after the suspensions are heated for 60 d at 70 °C (Table 1). Reduced  $\text{Zn}^{2+}$  solubility suggests its incorporation into the structure of the transformation products or, more likely, its movement within aggregates in a very porous ferrihydrite structure.

Cadmium solubility is approximately constant during 200 d of aging at room temperature (except for the slow titration after 200 d). Thermal treatment of

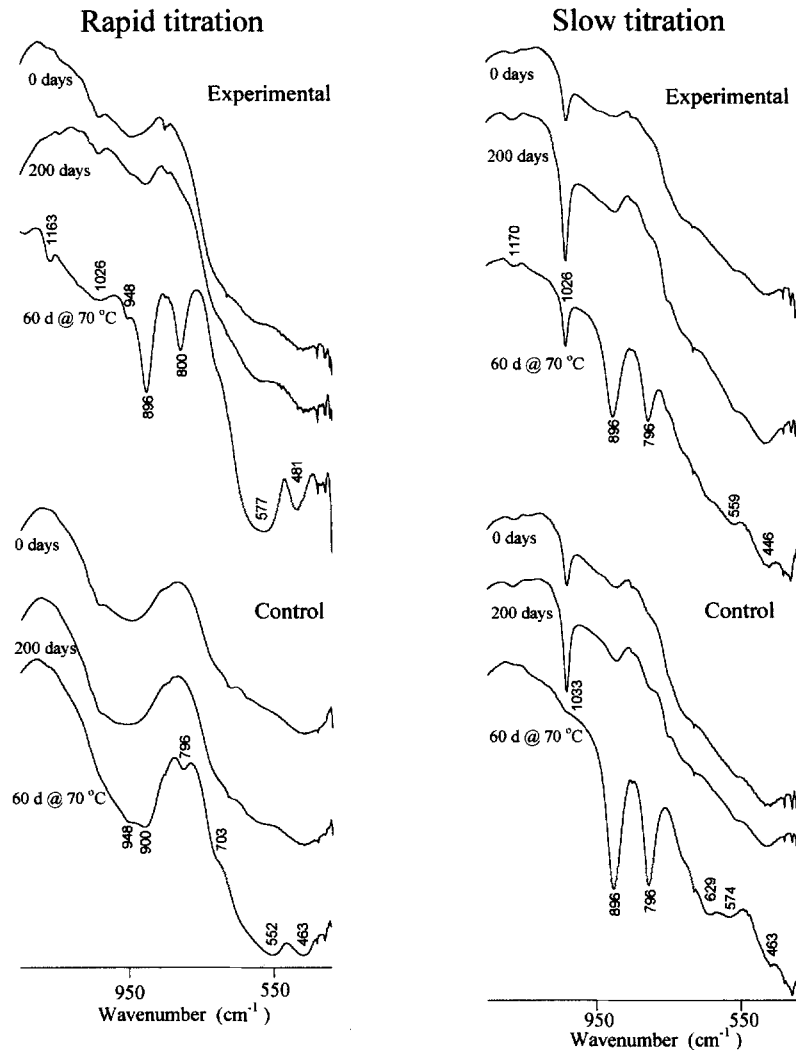


Figure 2. FTIR spectra of (co)precipitates taken immediately after their formation ( $t = 0$  d), after aging for 200 d at room temperature and after thermal treatment (60 d at 70 °C). Diagnostic IR bands ( $\text{cm}^{-1}$ ): goethite at 896 and 796; hematite at 570 and 480; lepidocrocite at 1170 and 1026.

Table 1. Concentration of  $\text{Cd}^{2+}$ ,  $\text{Cu}^{2+}$ ,  $\text{Pb}^{2+}$  and  $\text{Zn}^{2+}$  remaining in solution after aging the coprecipitates at room temperature for up to 200 d and after thermal treatment.

Time (d)	Metal solubility ( $\mu\text{M}$ ) <sup>†</sup>							
	Rapid titration				Slow titration			
	Zn	Cd	Pb <sup>‡</sup>	Cu	Zn	Cd	Pb <sup>‡</sup>	Cu
0	16.1	0.26	<5	0.31	10.5	0.33	<5	0.29
25	17.3	0.31	<5	2.04	10.4	0.28	<5	0.54
50	nd	nd	nd	nd	12.5	0.30	<5	0.65
75	17.6	0.28	<5	1.63	nd	nd	nd	nd
100	13.3	0.29	<5	0.71	11.4	0.33	<5	0.82
200	9.81	0.28	<5	0.58	7.01	0.16	<5	0.55
60 d at 70 °C	1.01	0.11	40	0.06	-0.06	0.007	20	0.76

<sup>†</sup> nd, not determined.

<sup>‡</sup> Pb measured at nM concentrations.

both rapid and slow titration coprecipitates produces a marked reduction in  $\text{Cd}^{2+}$  solubility (Table 1). In a previous study, a constant aqueous  $\text{Cd}^{2+}$  concentration was found during aging (17 d) and transformation of ferrihydrite to Gt (Ford et al. 1997). Other studies, however, have reported increased hysteresis in desorption of  $\text{Cd}^{2+}$  adsorbed onto freshly formed ferrihydrite after several weeks (Ainsworth et al. 1994) or its structural incorporation within the  $\alpha\text{-FeOOH}$  lattice upon coprecipitation (Spadini et al. 1994).

Lead solubility levels are below the limits of detection of dpa<sub>sv</sub> (5 nM) from 0 to 200 d of aging, but increase to 20–40 nM after heating the suspensions, indicating some ejection from the coprecipitates (Table 1). In a spectroscopic study, Manceau et al. (1993) suggested that as ferrihydrite transforms to more crystalline materials, the number of sorption sites for  $\text{Pb}^{2+}$  may decrease, resulting in a lower retention capacity. A  $\text{Pb}^{2+}$  coprecipitate may result in structural substitution of  $\text{Pb}^{2+}$  for  $\text{Fe}^{2+}$  initially (in a noncrystalline material). However, after aging and rearrangement of the solid phase, and because of the incompatibility of the ionic radius of  $\text{Pb}^{2+}$  with octahedral coordination,  $\text{Pb}^{2+}$  solubility can increase. Ford et al. (1997) reported that  $\text{Pb}^{2+}$  substituted into either the Gt/Hm structure but that it was expelled from the Fe oxide structure during aging.

Solubility values are much higher for  $\text{Cu}^{2+}$  during the first 75 d of aging the rapidly titrated coprecipitate (Table 1). Its solubility reaches a constant value after approximately 100 d of aging at room temperature (both rapid and slow titration). Thermal treatment (60 d at 70 °C) of the coprecipitate formed by rapid titration resulted in reduced  $\text{Cu}^{2+}$  solubility, while its solubility was virtually unchanged in the slowly titrated coprecipitate (Table 1). An increase in %  $\text{Cu}^{2+}$  removal from solution was observed by Kolthoff and Moskovitz (1937) after its coprecipitation with Fe at 25 °C followed by aging of the product at 98 °C for 70 min. No characterization of the solid phase was reported by the authors. Since  $\text{Cu}^{2+}$  has an ionic radius close to that of  $\text{Fe}^{3+}$ , it could be incorporated into the structure of a more crystalline product (such as Hm). A relatively constant  $\text{Cu}^{2+}$  solubility after aging and thermal treatment of the slow titration coprecipitate suggests a stable solid phase, but spectroscopic methods will be required to investigate these assumptions.

Aging and thermal transformation of ferrihydrite affect the solubility of coprecipitated metals. Solubility values resulting from these processes can limit metal toxicity and (bio)availability in soils. The solubilities of  $\text{Zn}^{2+}$  after thermal treatment are sufficiently low that they would be unlikely to be phytotoxic; however, it is not known if such mineral transformations occur in soil environments within realistic time frames. After aging,  $\text{Cd}^{2+}$  in solution represents a high percentage of the total concentration in the system (72% after rap-

id and 41% after slow titration). Even after thermal treatment, dissolved  $\text{Cd}^{2+}$  (in the rapid titration) is a substantial fraction of total  $\text{Cd}^{2+}$  in the system (28%), indicating that Fe oxides may not be reliable long-term sinks for  $\text{Cd}^{2+}$  in soils. Conversely, only 1.8% of the total  $\text{Cd}^{2+}$  remains in solution after thermal treatment of the slow titration product, but natural aging processes in soils may produce different results. If these transformation products were to form in soils, the measurable ejection of  $\text{Pb}^{2+}$  from the coprecipitates after thermal treatment would suggest that solid phases other than Fe oxides, such as phosphates or organic matter, may be more effective long-term sinks for  $\text{Pb}^{2+}$ . The level of dissolved  $\text{Cu}^{2+}$  after aging, and even after thermal treatment in the case of the slow titration, is sufficiently high that toxicity to biota and plants could be expected if these solubilities occurred in soils (Sauvé et al. 1995).

**METAL DISTRIBUTION.** By using SEM on freeze-dried samples, Fe oxides are seen as aggregates of very small particles which have a highly porous and granular structure (Figure 3). When seen at higher magnification, a granular-flat surface is evident but no definition is achieved (photograph not shown). EMPA is a direct method for determining the distribution of Zn and Cu in the Fe oxide aggregates. Cadmium and Pb distribution in the aggregates could not be determined; Cd concentration in/on the solid phase is too low, and Pb background signal is high and interferes with its accurate determination. Iron is also measured to ensure that a Fe oxide particle is analyzed. Line scan profiles provide information on the 1-dimensional spatial distribution of these elements (as shown in Figures 4 and 5). Analysis of several (10–15 per sample) Fe oxide aggregates show that high concentrations of Cu can be found at the edges of aggregates while Zn can be evenly distributed in the same aggregate (Figure 4). However, some aggregates show a lower concentration of Cu and/or Zn at the center than at the edges (Figures 5a and 5c), and yet others show areas randomly enriched or depleted in Cu and Zn concentrations (Figures 5b and 5d). Thus, line scans demonstrate that Zn and Cu: 1) segregate at the edge/periphery (since microprobe analysis looks at a flat surface) of some Fe oxide aggregates, 2) segregate within some aggregates, resulting in areas of elevated metal concentration, and 3) distribute evenly within some aggregates. No relationship is evident between type of segregation behavior and aging time or rate of coprecipitate formation. Since the aged coprecipitates comprise mixtures of microcrystalline and noncrystalline particles, and metals may be more concentrated in the less-crystalline particles (Nalovic et al. 1975), metal segregation within aggregates of particles is reasonable to expect.

Although experimental conditions (coprecipitation from homogeneous solution) provided the opportunity

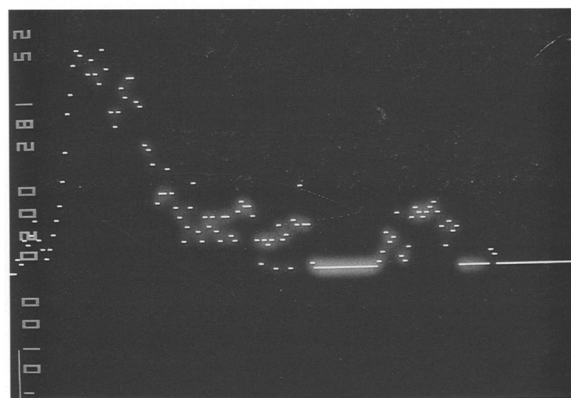
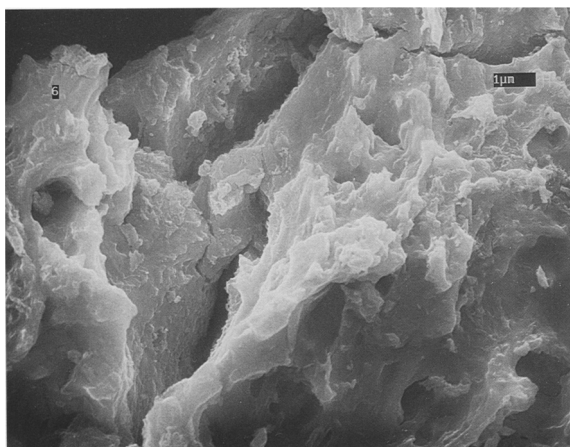
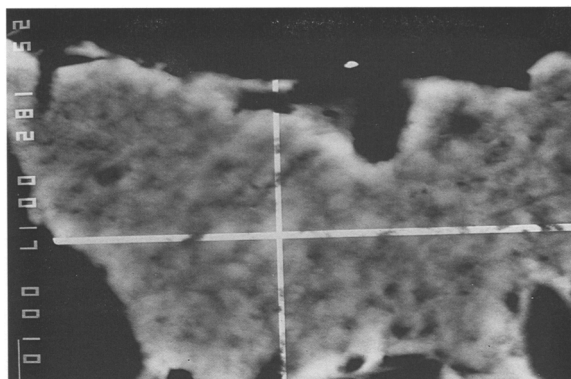
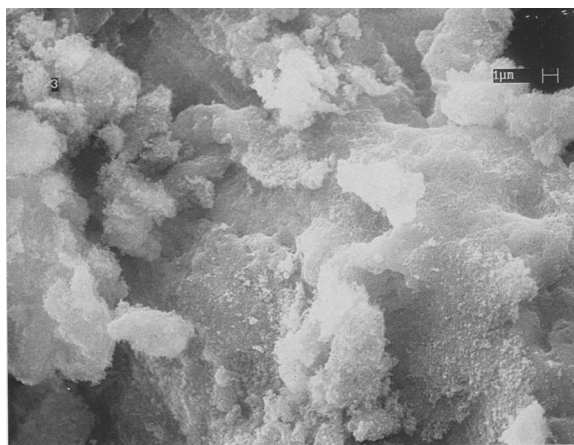


Figure 3. SEMs of the coprecipitates formed after heating the suspensions at 70 °C for 60 d. The samples are: 3, coprecipitate formed by rapid titration, and 6, coprecipitate formed by slow titration.

for metals to be sequestered and evenly distributed within the oxide structure, line scan profiles demonstrate the segregation of metals. By comparison, an EMPA of phosphate adsorption on ferrihydrate indicated that slow adsorption (after an initially rapid reaction) was the result of the time required for the phosphate to gain access to surface sorption sites located within aggregates of ferrihydrate particles (Willett et al. 1988). The authors proposed time-dependent phosphate adsorption as a result of diffusion within aggregates rather than solid-state diffusion. In the present study, however, this interpretation is not operative since experimental conditions provided “equal access” for metals to react with Fe oxides. Also, surface coverage by metals if they were concentrated at surfaces would be very low (from about 20–50 μmol

Figure 4. EMPA of an Fe oxide aggregate for a sample taken immediately after coprecipitate formation by rapid titration ( $t = 0$  d). a) Fe oxide aggregate, b) line scan of Cu and c) line scan of Zn. Line scans were taken along the horizontal line on (a). Horizontal lines on (b) and (c) are baseline levels resulting from cracks in the aggregate after application of 100 nA current.

$m^{-2}$ ; or 0.0069 mol  $M^{2+}$ /mol  $Fe^{3+}$ ) so that the “adsorption capacity” is well below its maximum. Metal segregation was indicated in an earlier work in which  $Cu^{2+}$  coprecipitation with Al hydroxide resulted in its

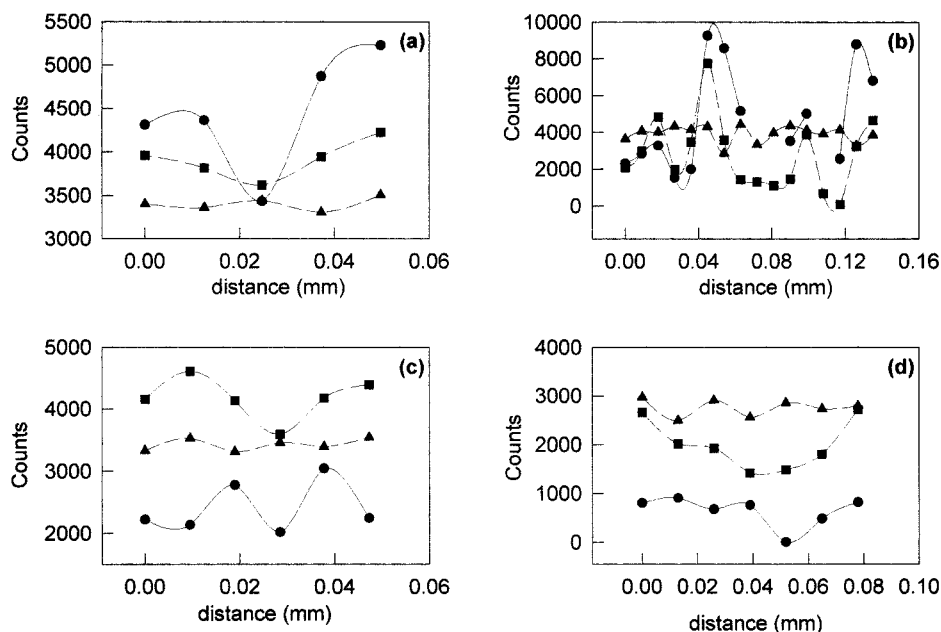


Figure 5. The distribution of Zn, Cu and Fe in Fe oxide aggregates. Iron counts  $\times 10^2$ , thus Fe concentration in the aggregates is considered constant. a) and b) two aggregates of different size, after rapid titration at  $t = 0$  d; c) after reaction for 200 d at room temperature (rapid titration); and d), after slow titration (at  $t = 0$  d). Symbols: ● for Zn, ■ for Cu and ▲ for Fe.

concentration at or very near the particle surfaces (McBride 1978). Consistent with coprecipitated metals concentrated near surfaces is their tendency to be preferentially retained in the less-crystalline (high surface area) fraction of oxide coprecipitates (Nalovic et al. 1975; Ford et al. 1997). Metal segregation within Fe oxides aggregates can influence metal solubility. If the oxide-bound metal is “buried” in the aggregate, the metal will be “protected” from going into solution; the opposite is true if the oxide-bound metal is located at the edge/periphery of the aggregate.

### CONCLUSIONS

Ferrihydrite phase transformation is affected by the rate of (co)precipitate formation (titration), and to a smaller degree by the presence of metals. The presence of a combination of heavy metals at a total level below 1 mole% promoted the formation of mixed end-products, some of which do not produce sharp XRD peaks and are considered to have microcrystalline structures. The rate of titration results in different products initially, as evidenced by XRD, which seems to influence the final end-products. For example, the rapid titration produces a noncrystalline, 1-line ferrihydrite while the slow titration results in a somewhat more ordered, 9-line ferrihydrite initially. The slow titration allows for organization of the Fe (hydr)oxide while the product is being formed, a product that is more stable upon subsequent aging. This more ordered initial product is stable even after heating the sample at 70 °C for 60 d.

It is known that nuclei promoting the formation of Hm form during rapid titration.

Aging and thermal-mediated transformation of ferrihydrite affect solubility of coprecipitated metals. Cadmium and  $Zn^{2+}$  solubility decrease after thermal treatment while  $Pb^{2+}$  solubility increases. This behavior may be the result of metal movement into or out of a porous material rather than to structural incorporation, whereas the latter seems more reasonable in explaining  $Cu^{2+}$  solubility. Although  $Cu^{2+}$  solubility appeared to respond to pH changes during aging at room temperature (Martínez and McBride 1998), its solubility after thermal treatment seems to respond (at least partially) to structural changes in the coprecipitate. Copper has an ionic radius close to that of  $Fe^{3+}$ , so it could be incorporated into the structure of a crystalline Fe oxide, such as Hm. Although experimental conditions provided for the homogeneous distribution of metals within the Fe oxide structure and/or aggregates, electron microprobe analysis indicates some degree of segregation.

### ACKNOWLEDGMENTS

This research was supported by the USDA-NRI Competitive Grants Program, award no. 95-37107-1620.

### REFERENCES

- Ainsworth CC, Pilon JL, Gassman PL, Van Der Sluys WG. 1994. Cobalt, cadmium, and lead sorption to hydrous iron oxide: Residence time effects. *Soil Sci Soc Am J* 58:1615–1623.



- Anderson PR, Benjamin MM. 1985. Effects of silicon on the crystallization and adsorption properties of ferric oxides. *Environ Sci Technol* 19:1048–1053.
- Cornell RM. 1988. The influence of some divalent cations on the transformation of ferrihydrite to more crystalline products. *Clay Miner* 23:329–332.
- Cornell RM, Giovanoli R. 1987. Effect of manganese on the transformation of ferrihydrite into goethite and jacobite in alkaline media. *Clays Clay Miner* 35:11–20.
- Cornell RM, Giovanoli R. 1988. The influence of copper on the transformation of ferrihydrite ( $5\text{Fe}_2\text{O}_3 \cdot 9\text{H}_2\text{O}$ ) into crystalline products in alkaline media. *Polyhedron* 7:385–391.
- Cornell RM, Giovanoli R. 1989. Effect of cobalt on the formation of crystalline iron oxides from ferrihydrite in alkaline media. *Clays Clay Miner* 37:65–70.
- Cornell RM, Schneider W, Giovanoli R. 1989. The transformation of ferrihydrite into lepidocrocite. *Clay Miner* 24:549–553.
- Crawford RJ, Harding IH, Mainwaring DE. 1993. Adsorption and coprecipitation of single heavy metal ions onto the hydrated oxides of iron and chromium. *Langmuir* 9:3050–3056.
- Ford RG, Bertsch PM, Farley KJ. 1997. Changes in transition and heavy metal partitioning during hydrous iron oxide aging. *Environ Sci Technol* 31:2028–2033.
- Kinniburgh DG, Jackson ML, Syers JK. 1976. Adsorption of alkaline earth, transition, and heavy metal cations by hydrous oxide gels of iron and aluminum. *Soil Sci Soc Am J* 40:796–799.
- Kolthoff IM, Moskovitz B. 1937. Studies on coprecipitation and aging. XI. Adsorption of ammonio copper ion on and coprecipitation with hydrous ferric oxides. Aging of the precipitate. *J Phys Chem* 41:629–644.
- Manceau A, Charlet L, Boisset MC, Didier B, Spadini L. 1993. Sorption and speciation of heavy metals on hydrous Fe and Mn oxides: From microscopic to macroscopic. *Appl Clay Sci* 7:201–223.
- Martínez CE, McBride MB. 1998. Solubility of  $\text{Cd}^{2+}$ ,  $\text{Cu}^{2+}$ ,  $\text{Pb}^{2+}$ , and  $\text{Zn}^{2+}$  in aged coprecipitates with amorphous iron hydroxides. *Environ Sci Technol* 32:743–748.
- McBride MB. 1978. Retention of  $\text{Cu}^{2+}$ ,  $\text{Ca}^{2+}$ ,  $\text{Mg}^{2+}$ , and  $\text{Mn}^{2+}$  by amorphous alumina. *Soil Sci Soc Am J* 42:27–31.
- Nalovic LJ, Pedro G, Janot C. 1975. Demonstration by Mössbauer spectroscopy of the role played by transitional trace elements in the crystallogenesis of iron hydroxides (III). In: Bailey SW, editor. *Proc Int Clay Conf*. Wilmette, IL: Applied Publishing. p 601–610.
- Sauve S, McBride MB, Hendershot WH. 1995. Ion-selective electrode measurements of copper (II) activity in contaminated soils. *Arch Environ Contam Toxicol* 29:373–379.
- Schwertmann U, Murad E. 1983. Effect of pH on the formation of goethite and hematite from ferrihydrite. *Clays Clay Miner* 31:277–284.
- Schwertmann U, Taylor RM. 1989. Iron oxides. In: Dixon JB, Weed SB, editors. *Minerals in soil environments*. Madison, WI: Soil Sci Soc Am. p 379–438.
- Spadini L, Manceau A, Schindler PW, Charlet L. 1994. Structure and stability of  $\text{Cd}^{2+}$  surface complexes on ferric oxides 1. Results from EXAFS spectroscopy. *J Colloid Interface Sci* 168:73–86.
- Willett IR, Chartres CJ, Nguyen TT. 1988. Migration of phosphate into aggregated particles of ferrihydrite. *J Soil Sci* 39:275–282.

(Received 2 September 1997; accepted 23 January 1998; Ms. 97-085)